Atmospheric Environment 45 (2011) 5440–5449

Contents lists available at ScienceDirect

Atmospheric Environment

journal homepage: www.elsevier.com/locate/atmosenv

Sources of mercury in precipitation to Underhill, VT

Lynne E. Gratz*, Gerald J. Keeler

University of Michigan Air Quality Laboratory, 1415 Washtenaw Heights, SPH 1-Tower, Ann Arbor, MI 48109-2029, USA

ARTICLE INFO

Article history:
Received 14 March 2011
Received in revised form
29 June 2011
Accepted 3 July 2011

Keywords:
Mercury
Precipitation
Trace elements
Source apportionment
Receptor modeling

ABSTRACT

Daily event precipitation samples were collected from 1995 to 2006 in Underhill, VT, USA and analyzed for mercury (Hg) and trace elements. Over the 12-year period, annual Hg deposition levels at Underhill did not decline significantly despite regulatory efforts to reduce Hg emissions in the United States. Mercury and trace element wet deposition data were examined using the multivariate receptor model EPA PMF 3.0 to identify the sources contributing to Hg deposition at the Underhill site. Results indicate that coal combustion, a mixture of incineration and non-ferrous metal smelting, and a phosphorus source contributed to the observed Hg wet deposition. The model consistently indicated that coal combustion contributed ~60% of the total Hg measured in wet deposition and the contribution from this source did not change significantly over time. Mercury and trace element deposition were further analyzed using a hybrid-receptor model, quantitative transport bias analysis (QTBA), to identify the likely source locations contributing to Hg deposition. Results from QTBA indicate that the majority of Hg deposition at Underhill is due to transport from the Midwestern United States, where the density of coal-fired utility boilers in the U.S. is largest.

1. Introduction

Mercury (Hg) is a persistent hazardous air pollutant and bioaccumulative neurotoxin. Atmospheric deposition is widely recognized as a dominant mechanism by which Hg enters terrestrial and aquatic ecosystems (Landis and Keeler, 2002; Hammerschmidt and Fitzgerald, 2006) where, upon conversion to the organic form methylmercury, it can bioaccumulate within the food chain (Schroeder and Munthe, 1998). Investigating atmospheric Hg emissions and transport pathways is critical for mitigating its environmental impact.

Mercury exists in the atmosphere predominantly as gaseous elemental Hg (Hg^0), fine particulate bound Hg (Hg_p), and divalent reactive gaseous Hg (RGM). Elemental mercury is relatively stable and able to travel long distances before being converted to the more soluble divalent forms (Hg_p and RGM; or Hg(II)) that deposit readily (Schroeder and Munthe, 1998; Lin and Pehkonen, 1999). Consequently, Hg can be transported locally, regionally, and globally and Hg deposition at any location may represent a complex mixture of source emissions and atmospheric processes.

Underhill, VT, USA is a remote location where elevated levels of Hg in the region's fish and wildlife remain a critical issue (Hammerschmidt and Fitzgerald, 2006; Evers et al., 2007) despite efforts to reduce regional Hg emissions. Previously, municipal and medical waste incinerators were considered one of the largest anthropogenic sources of atmospheric Hg; however, following the 1990 Clean Air Act Amendments the U.S. EPA imposed nationwide restrictions on waste incinerator stack emissions (U.S. EPA, 1997; NESCAUM, 2005). By 1999, the targeted 95% reduction in waste incinerator Hg emissions had largely been met (Cohen et al., 2007). In the northeast, where municipal waste incineration once accounted for ~55% of the estimated Northeast Regional Mercury Emissions Inventory (NEIWPCC, 2007), emissions from municipal and medical waste incinerators declined by ~70% between 1998 and 2002 (NESCAUM, 2005). Yet despite these regulatory successes, annual Hg wet deposition at Underhill did not decline significantly between 1995 and 2006 as transport from the industrialized Midwest and urban East Coast corridor consistently contributed to the largest observed Hg wet deposition amounts (Gratz et al., 2009). These findings suggest that additional regional emission sources contributed to Hg deposition at Underhill.

In fact, fossil fuel combustion remains the largest anthropogenic Hg source in the U.S. because emissions, such as those from coal-fired utility boilers (CFUBs), have not declined substantially over time (Cohen et al., 2007; Butler et al., 2008). CFUB emission reductions were anticipated under U.S. EPA's cap-and-trade approach proposed in the 2005 Clean Air Mercury Rule (Cohen et al., 2007). However, this rule was overturned in 2008 when

* Corresponding author. Present address: CNR-Institute of Atmospheric Pollution Research, c/o UNICAL-Polifunzionale, 87036 Rende, Italy. Tel.: +39 0984 493250.
E-mail addresses: lgratz@umich.edu, l.gratz@iia.cnr.it (L.E. Gratz).

1352-2310/$ – see front matter © 2011 Elsevier Ltd. All rights reserved.
doi:10.1016/j.atmosenv.2011.07.001

states and other parties encouraged the use of more stringent maximum achievable control technologies (MACT), as stipulated in the 1990 Clean Air Act Amendments. In light of these efforts to regulate Hg emissions and the observed temporal patterns in Hg wet deposition, the Underhill dataset presents a unique opportunity to study source contributions to Hg deposition over time.

Multivariate statistical receptor models are widely used in air quality studies to determine the sources of atmospheric constituents. Previous applications of positive matrix factorization (PMF) to aerosol concentrations at Underhill indicated that fossil fuel combustion, local wood smoke, and secondary sulfate production were the dominant sources of $PM_{2.5}$ mass to the site (Polissar et al., 2001; Poirot et al., 2001; Gao et al., 2006). Municipal waste incineration was identified as a major source from 1988 to 1995 (Polissar et al., 2001), but could not be identified as a stand-alone source in 2001–2003, likely due to emission reductions (Gao et al., 2006). The application of receptor models to aerosol measurements at other U.S. Midwest and East Coast locations also demonstrated the regional influence of industrial sources (e.g. coal- and oil-fired utility boilers, iron–steel manufacturing) (Olmez et al., 1998; Liu et al., 2003; Morishita et al., 2006; Hammond et al., 2008). Given the pattern of Hg transport from the Midwest and East Coast (Gratz et al., 2009), wet deposition at Underhill is likely influenced by these regional sources.

The application of receptor models to precipitation data is complex given that the wet removal of atmospheric constituents may vary with aerosol size fraction, distance between source and receptor, meteorological conditions and atmospheric chemistry during transport. However, the chemical compositions and elemental ratios of many pollutants are reasonably well preserved during transport (Keeler and Samson, 1989; Rahn and Lowenthal, 1984) suggesting that statistical models can be applied to precipitation data as long as the atmospheric behavior of measured species are considered. PMF has been successfully applied to precipitation data to determine the sources of Hg and other trace elements (Juntto and Paatero, 1994; Anttila et al., 1995; Keeler et al., 2006).

In this study we applied the multivariate statistical receptor model EPA PMF 3.0 to 12 years of Hg and trace element precipitation measurements to identify the sources contributing to Hg wet deposition at Underhill. Additionally we utilized a trajectory-based hybrid-receptor model, quantitative transport bias analysis (QTBA), to determine the locations of the identified source emissions.

2. Methodology

2.1. Sample collection and analysis

The Underhill site is ~25 km east of Lake Champlain on the west slope of Mount Mansfield (elevation 399 m) (Fig. 1). Daily event wet-only precipitation samples were collected for Hg and trace element analysis using a modified MIC-B (MIC, Thornhill, Ontario) automatic precipitation collector (Landis and Keeler, 1997). Separate sampling trains for Hg and trace elements (Keeler et al., 2005; Gratz et al., 2009) were prepared at the University of Michigan Air Quality Laboratory (UMAQL) (Landis and Keeler, 1997) to ensure that they were Hg- and trace element-free prior to use. Site operators replaced sampling trains after daily precipitation events. Precipitation events > 0.10 cm were used in the subsequent data analysis. The volume of each precipitation sample was determined gravimetrically. Precipitation depths were determined using the Hg funnel area (191 cm^2).

Following collection, Hg samples were oxidized with concentrated BrCl to a 1% solution (v/v) and stored for at least 24 h in a dark cold room prior to Hg concentration analysis by cold-vapor atomic fluorescence spectrometry (CVAFS) (Landis and Keeler,

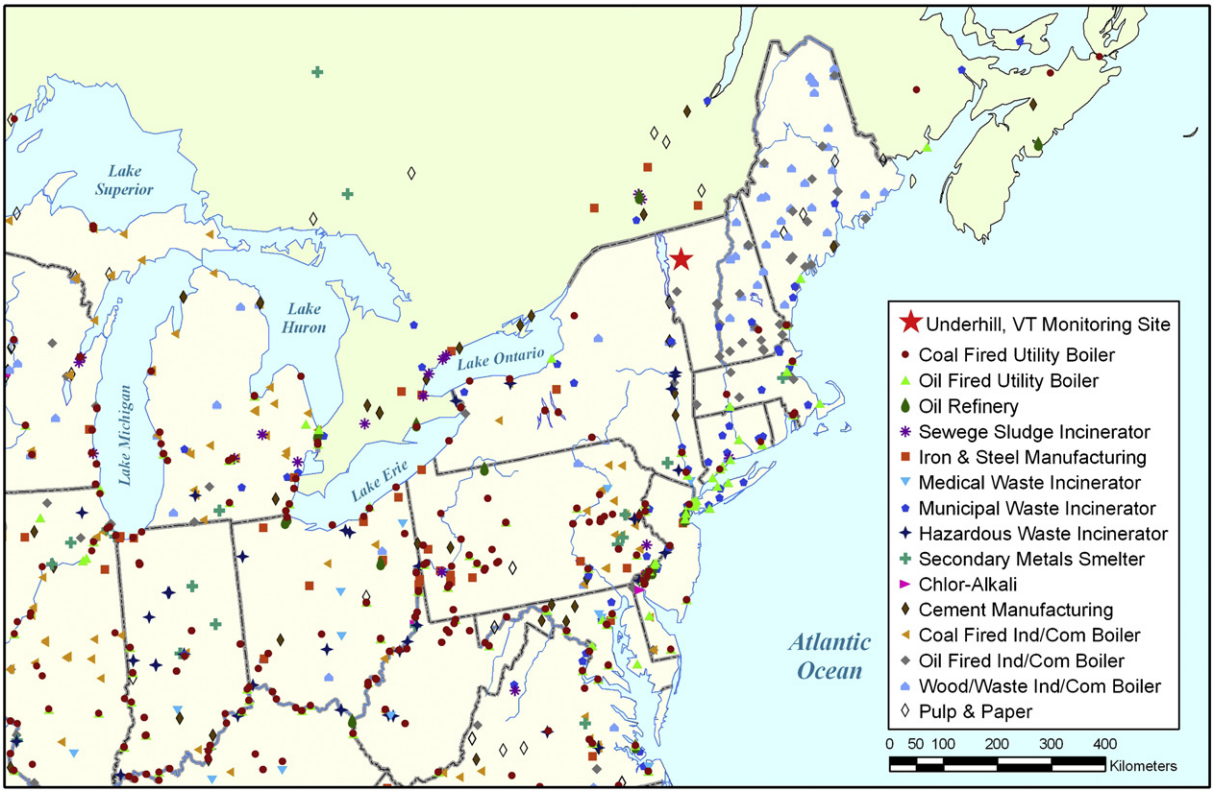

Fig. 1. Location of the Underhill, VT monitoring site and major mercury point sources emitting ≥0.1 kg yr^{-1} (U.S. EPA, 2005; Environment Canada, 2007). U.S. sources correspond to the MACT source category.

1997; Keeler et al., 2005). Trace element samples were acidified with concentrated HNO_3 to a 0.2% solution (v/v) and stored in a dark cold room for a minimum of two weeks to permit the desorption of trace elements from particles and from the walls of the collection bottle (Landis and Keeler, 1997). Samples were analyzed for a suite of trace element concentrations using a Finnigan MAT Element magnetic sector high resolution inductively coupled plasma mass spectrometer (ICP-MS) (Table SI-1).

2.2. Multivariate statistical receptor modeling

Positive Matrix Factorization (PMF) is a weighted least-squares model which decouples measured data values into two factor matrices representing the estimated source profile and source contributions to each sample (Paatero and Tapper, 1994; Paatero, 1997). The source profile represents the mean deposition amount for each analyte in each factor (Paatero and Tapper, 1994) and can be interpreted using previously reported source compositions. The source contribution matrix contains the loadings of each factor to each individual sample. Data values in PMF are individually weighted by their uncertainties (Paatero, 1997). PMF imposes non-negativity constraints on the modeled contributions to individual elements given the physical reality of the source–receptor problem (e.g. no source can contribute negative mass of a given element) (Paatero, 1997; Norris et al., 2008).

PMF determines a residual matrix comprised of the difference between measured and modeled values, and then weights the residuals using the measurement uncertainties. PMF calculates a goodness-of-fit parameter (Q) based upon the weighted residuals and tries to minimize Q with respect to the factor matrices while imposing the non-negativity constraints (Paatero, 1997).

We converted the measured elemental concentrations to deposition using the measured precipitation depth prior to input to the model. We replaced elemental concentrations less than zero with one half of the method detection limit (MDL) (Table SI-1). Sample uncertainties were calculated using the MDL, sample collection uncertainty ($SC = 10\%$), analytical measurement uncertainty (AM = standard deviation of three replicate analysis for each sample), and precipitation depth measurement uncertainty ($PD = 5\%$) (Keeler et al., 2006).

$$U = (MDL) + \sqrt{(SC)^2 + (AM)^2 + (PD)^2} \quad (1)$$

The variability in the PMF solution was estimated using a block bootstrap technique that calculates the stability of the model output by randomly re-sampling blocks of the input dataset and computing the variability between model solutions (Norris et al., 2008). The elemental contributions to each factor were deemed significant when the fifth percentile of the bootstrap uncertainty was greater than zero (Keeler et al., 2006).

Initially, we applied PMF to the full 12 years of wet deposition measurements, and then separately to two six-year periods (1995–2000, 2001–2006) to explore temporal variability in the source contributions.

2.3. Meteorological trajectory analysis

Three-day back trajectories were calculated using the Hybrid Single-Particle Lagrangian Integrated Trajectory (HYSPLIT) Model Version 4.8 (Draxler and Hess, 1997). Gridded meteorological data was obtained from the NOAA Air Resources Laboratory (ARL) using the National Center for Environmental Prediction (NCEP) Nested Grid Model (NGM) (1995–1996) and the Eta Data Assimilation System (EDAS) (1997–2006). We used the hour of maximum precipitation, determined by the onsite tipping bucket rain gauge, as the starting time for each event. Trajectory starting heights were set to one half of the mixed layer depth, as determined by the HYSPLIT model.

2.4. Quantitative transport bias analysis (QTBA)

QTBA is a trajectory-based hybrid-receptor model that combines air mass back trajectories with measured amounts of analytes at the receptor site to determine the most probable source regions of pollutants (Keeler and Samson, 1989). QTBA defines the probability of a particular species arriving at the receptor location (x, y) at time (t) as:

$$A(x,t) = \int_{t-\tau}^{t} \int_{-\infty}^{\infty} \int_{-\infty}^{\infty} T(x,y,t|x',y',t')\,dx'\,dy'\,dt' \quad (2)$$

where the potential mass transfer function, $T(x,y,t|x',y',t')$ is defined by:

$$T(x,y,t|x',y',t') = Q(x,y,t|x',y',t')R(x,y,t|x',y',t') \\ D(x,y,t|x',y',t')\Lambda(x,y,t|x',y',t') \quad (3)$$

$Q(x,y,t|x',y',t')$ is the transition probability density function of an air parcel arriving at the site at a given time. QTBA assumes that Q is normally distributed about the trajectory axis with a standard deviation that increases linearly upwind due to atmospheric dispersion (Keeler and Samson, 1989). $R(x,y,t|x',y',t')$ is the probability that the species will not react to form another species during transport. We assumed this to be 100%, which is a suitable approximation for Hg^0, Hg_p (Burke, 1998; Liu, 2007) and trace elements (Keeler and Samson, 1989). This may not be suitable for RGM (Liu, 2007); however, we assumed that Hg transported to Underhill was predominantly Hg^0 prior to oxidation and removal through precipitation. $D(x,y,t|x',y',t')$ and $\Lambda(x,y,t|x',y',t')$ are the probabilities that the species will not be dry or wet deposited during transport. We assumed that they were linearly proportional to the measured deposition amounts (Keeler and Samson, 1989; Liu, 2007). We estimated the dry deposition rate coefficient as a ratio between the dry deposition velocity and the mixing height (Keeler and Samson, 1989). Dry deposition velocity was allowed to vary diurnally and seasonally (Keeler and Samson, 1989; Burke, 1998; Liu, 2007), and the mixing height along each trajectory was determined in the HYSPLIT model. The wet deposition rate coefficient was approximated according to the power law $Precipitation^{0.6}$ (Keeler and Samson, 1989) and precipitation amounts along the trajectory path were obtained from HYSPLIT gridded meteorological data.

Integration of $T(x,y,t|x',y',t')$ generates a transport probability field, $T_k(x,y,t|x',y',t')$, for each trajectory k. Each transport probability field is weighted by the associated deposition amount producing a weighted potential mass transfer field $T_w(x,y,t|x',y',t')$ (Keeler and Samson, 1989). The QTBA field is defined as the ratio of weighted to un-weighted potential mass transfer fields multiplied by the average deposition amount for the study period (Liu, 2007). The QTBA field has units of deposition and is viewed as 2-dimensional contours depicting the most probable regions associated with elevated deposition amounts.

Similar trajectory-based models, such as potential source contribution function (PSCF) or residence-time weighted concentrations (RTWC), compare the residence time of trajectories in each grid cell with measured concentrations to determine emission source locations (Zhou et al., 2004). These models rely on the accuracy of trajectories and assume that time spent in a given grid cell is directly related to the measured concentration. Instead, QTBA

uses a 2-dimensional normal distribution to calculate the probability of a measured species being transported from a given direction. QTBA also accounts for increasing uncertainty in the computed trajectory with distance from the receptor site (Kahl and Samson, 1986) and for wet and dry deposition along the trajectory path, which can lower the probability of transport. The inclusion of these uncertainties makes QTBA a powerful tool for examining source–receptor relationships.

2.5. Preliminary data analysis

Between 1995 and 2006, 1155 precipitation samples were collected at Underhill (Gratz et al., 2009) and 1096 contained sufficient volumes for analysis in both the Hg and trace element sampling trains. Initially we examined the Hg and trace element data using principle component factor analysis (PCA) with Varimax rotation and Kaiser Normalization (SPSS v16) to estimate the source profiles and identify potential sample outliers. The data distributions suggested that samples with PCA factor scores >5 or <−5 were extreme outliers that strongly influenced the data and source profiles. These outliers (41 samples; 3.7% of the combined Hg and trace element dataset) were removed before analysis with PMF and QTBA. One of the removed events was an extreme outlier for Hg deposition and was explored in detail by Keeler et al. (2005). Summary statistics for the Hg and trace element samples included in PMF and QTBA are presented in Table 1.

3. Results

3.1. PMF of 1995–2006 data

PMF resolved a five factor solution (Table 2; Fig. 2) which we identified as: (1) mixed smelter and incinerator, (2) oil combustion, (3) phosphorus, (4) iron–steel manufacturing, and (5) coal combustion. Based upon the bootstrapping analysis and the relative attribution of Hg deposition to each factor, three of five source categories contributed significantly to Hg deposition: smelter/incinerator (12.7%), phosphorus (26.5%), and coal combustion (60.7%) (Fig. 3). PMF reproduced 78% of the total measured Hg deposition. The remaining 22% may represent sources of Hg not accounted for by the model, such as contributions from the global background or re-emitted Hg. A regression of PMF observed versus predicted Hg values had a slope of 0.63, an intercept of 0.02, and an R^2 of 0.68 (Table SI-2). The scaled residuals for Hg were normally distributed, which suggested that Hg deposition was effectively modeled in PMF (Norris et al., 2008).

Table 1
Summary statistics of Hg and trace element wet deposition (μg m^{-2}) for all samples included in the PMF and QTBA models (n = 1055).

Element	Mean	Median	Standard Deviation
Mg	255	164	277
Al	278	150	369
P	78.6	48.0	94.7
S	5928	3489	7215
K	348	203	484
V	2.47	1.66	2.76
Cr	0.86	0.57	1.02
Mn	24.1	12.2	38.0
Fe	245.6	135.3	312.6
Co	0.25	0.16	0.28
Cu	22.4	11.8	31.5
Zn	59.9	39.1	74.6
As	1.12	0.79	1.10
Se	2.05	1.21	2.38
Sr	4.25	2.80	4.88
Cd	0.59	0.40	0.74
La	0.28	0.16	0.35
Ce	0.48	0.24	0.67
Hg	0.10	0.07	0.10
Pb	6.31	4.02	7.00

Table 2
PMF source factor profiles (μg m^{-2}) for Underhill precipitation samples (1995–2006). The highest contribution from each element is shown in bold.

	Smelter/ Incinerator	Oil Combustion	Phosphorous	Iron–Steel	Coal Combustion	% of Deposition Explained
Mg	26.2	6.8	57.2	**108.4**	28.3	89%
Al	*	*	*	**160**	*	58%
P	*	*	**64**	*	*	82%
S	*	1173	72	*	**4165**	91%
K	*	*	**160.0**	*	49.9	61%
V	*	**1.39**	*	*	*	57%
Cr	0.14	0.20	0.11	**0.23**	*	79%
Mn	*	*	3.07	**8.00**	*	46%
Fe	*	*	20	**160**	22	82%
Co	0.03	0.04	0.02	**0.09**	0.03	87%
Cu	**11.3**	*	2.1	*	*	60%
Zn	**18.7**	12.9	8.4	*	2.3	71%
As	0.20	0.29	0.07	0.08	**0.31**	86%
Se	*	0.52	*	*	**1.21**	84%
Sr	0.88	0.24	0.49	**1.80**	0.40	90%
Cd	**0.18**	0.15	0.07	*	*	70%
La	0.02	0.02	*	**0.16**	0.04	89%
Ce	*	*	*	**0.32**	0.06	81%
Hg	0.01	*	0.02	*	**0.05**	78%
Pb	**2.9**	1.09	*	*	0.9	78%
% Hg	12.7%	*	26.5%	*	60.7%	

*Not significant at 95% confidence interval.

3.2. PMF of 1995–2000 and 2001–2006 data

From 1995 to 2000, PMF identified the same five factors and comparable trace element loadings as those identified in the 12-year dataset (Table SI-3). Source factor contributions to Hg deposition were significant from smelter/incinerator (26.0%), phosphorus (8.6%), and coal combustion (57.1%). PMF attributed a small amount of Hg deposition to iron–steel manufacturing, but the contribution (8.2%) was insignificant according to the bootstrap analysis.

From 2001 to 2006, PMF calculated four factors: smelter/incinerator, phosphorus, iron–steel manufacturing, and coal combustion (Table SI-4). Hg deposition was significantly attributed to the phosphorus (30.4%) and coal combustion (64.7%) sources. The contributions from smelter/incinerator (3.7%) and iron–steel (1.2%) were insignificant.

3.3. QTBA

We modeled select trace elements (Pb, V, P, Fe, Se, S) (Fig. 4) representing the PMF source factors and compared the model output with the known locations of major emission sources (Fig. 1) to confirm that QTBA could effectively identify the likely source regions. We then modeled the measured Hg wet deposition (Fig. 5). Finally, we applied QTBA to the PMF estimated contributions to event Hg deposition from each source factor (Fig. 6).

4. Discussion

4.1. PMF

The mixed smelter/incinerator factor contained the highest loadings of Cd, Zn, Pb, and Cu. PMF did not calculate distinct smelter

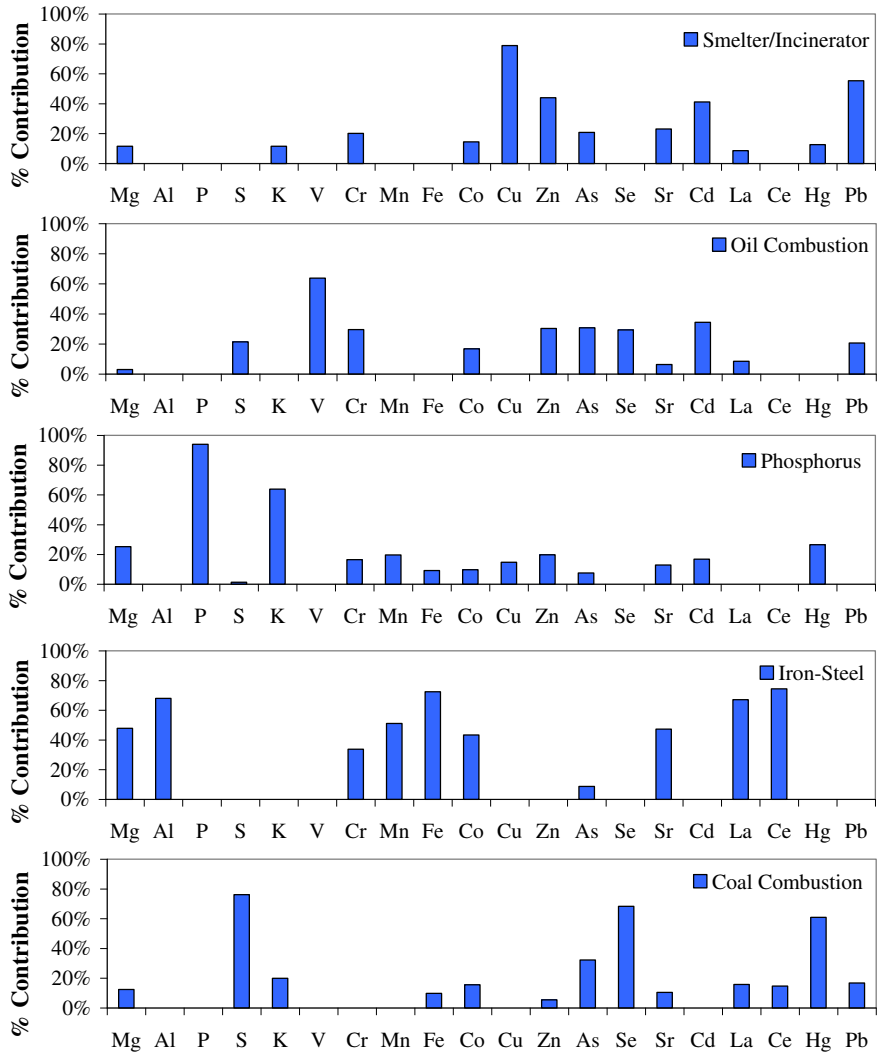

Fig. 2. Percent of the total modeled deposition of each element attributed to the PMF factors.

and incinerator sources, likely due to common elements in their emissions and the presence of other upwind anthropogenic sources emitting similar elements (e.g. cement production) (Polissar et al., 2001). This idea was further supported by the elemental ratios. Most Underhill samples displayed Zn/Pb ratios well above a previously suggested ratio (1.8) for municipal waste incinerator emissions (Fig. SI-1; Olmez et al., 1988), and the Zn/Pb ratio on the smelter/incinerator factor was 6.5. However, the Zn/Pb ratio previously reported for mixed incineration/smelting in Underhill aerosols was also ~3.5 times greater than the Olmez et al. (1988) ratio due to Pb reductions in many products and the mixing of smelter and incineration source emissions during upwind transport (Polissar et al., 2001). The smelter/incinerator contribution to Hg wet deposition was greatest in the winter (21%) and lowest in the summer (11%) (Fig. 3). Additionally, precipitation events with As/Se $>$ 1 (signifying smelter emissions (Olmez et al., 1998)), occurred more often during winter months under northerly flow, indicating the wintertime impact of Canadian smelters (Olmez et al., 1998; Polissar et al., 2001). Only 23% of samples contained As/Se $>$ 1 (Fig. SI-3); however, a reduced smelter influence on $PM_{2.5}$ mass was also previously observed at Underhill between the 1988–1995 and 2001–2003 PMF analyses, perhaps suggesting the effect of emission controls on Canadian non-ferrous smelters (Gao et al., 2006). Mercury wet deposition measured in precipitation samples with As/Se $>$ 1 accounted for only 16% of the total Hg wet deposition during the 12-year period. Furthermore, while smelting/incineration was a significant source of Hg from 1995 to 2000 (Table SI-3), PMF no longer identified a contribution to Hg deposition from smelting/incineration from 2001 to 2006 (Table SI-4). This was consistent with reduced Hg emissions from incinerators during the study period.

The oil combustion factor had the highest loading of V with additional contributions from Cd, S, Cr, Zn, As, and Se. Vanadium is a key tracer element that is dominantly emitted from oil combustion sources, including oil-fired power plants and residual oil burning (Mamane and Pirrone, 1998). Oil combustion did not contribute significantly to Hg deposition, consistent with our understanding that much lower Hg concentrations are found in residual oil than in coal burned in utility boilers (Olmez et al., 1998). The La/V ratios in the Underhill samples demonstrated seasonal variability, suggesting increased residual oil burning during fall/winter in the Northeast for power generation and heating (Fig. SI-2). However, Hg deposition amounts were substantially lower during winter due, in part, to inefficient scavenging of atmospheric Hg(II) by snowfall (Burke et al., 1995; Gratz et al., 2009); thus an insignificant contribution from oil combustion to Hg wet deposition is reasonable. With respect to the

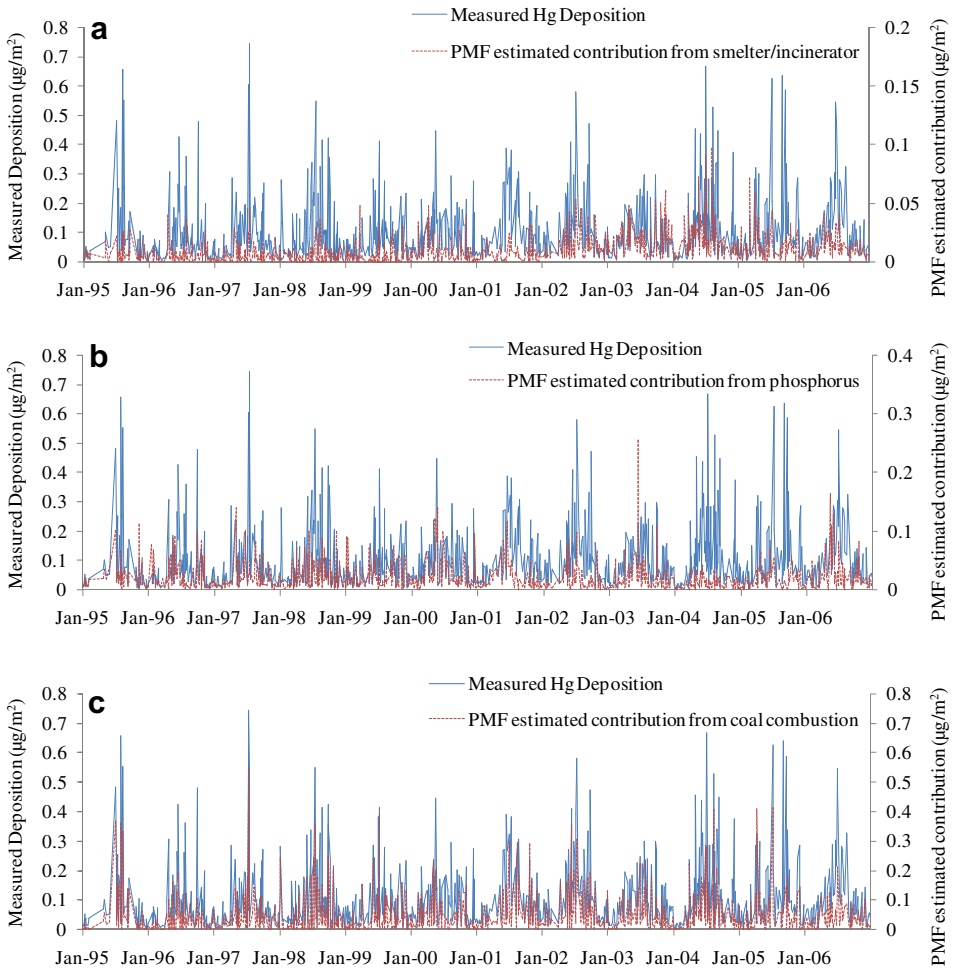

Fig. 3. Time series of measured Hg wet deposition (μg m^{-2}) compared to the PMF estimated contributions to Hg wet deposition (μg m^{-2}) from (a) smelter/incinerator, (b) phosphorus, and (c) coal combustion sources.

two 6-year analyses, PMF did not identify a factor resembling oil combustion in 2001–2006; however, the total measured V deposition was ~20% lower in 2001–2006 than in 1995–2000, perhaps suggesting a decline in residual oil burning influences.

The phosphorus source contained significant contributions from P, Mg, Mn, and K. The high P and K loadings could represent biomass burning sources (Mahowald et al., 2008), which in the northeastern U.S. include wood-fired commercial/industrial boilers, residential wood burning, and/or forest fires (Polissar et al., 2001). Wood smoke with high loadings of K contributed significantly to $PM_{2.5}$ at the Underhill site, with the largest source contributions occurring in winter/spring under northerly flow (Polissar et al., 2001). Alternatively, the phosphorus factor could represent wood-fired boiler, paper mill, and/or wastewater treatment plant waste used as fertilizer to enrich soils with P and K (Vance, 1996; Pitman, 2006). In the U.S. most boiler ash and wastewater sewage sludge is sent to landfills or incinerated, but, in the Northeast ~80% is converted to "biosolids" and other organic residuals that are land-applied as fertilizer (Erich and Ohno, 1992; Vance, 1996). Although the phosphorus factor did not contain significant contributions from common crustal elements (e.g. La, Ce) that would suggest transport of windblown soil particles, primary biogenic emissions are a known atmospheric source of P and K (Mahowald et al., 2008) and the consistent relationship between Hg, P, and K may suggest that vegetation treated with biosolids is an important regional source. The phosphorus source contribution to Hg wet deposition varied seasonally, contributing ~30% in the spring, fall, and winter and ~19% in the summer (Fig. 3). This may be explained by seasonal variability either in emissions from the aforementioned sources or in transport pathways to the site.

The iron–steel manufacturing factor displayed high loadings of Fe along with Mg, Cr, Mn, Al, and Co (Machemer, 2004). Elevated Al loadings may also reflect emissions from Midwestern Al production facilities (U.S. EPA, 2002 NEI) located near major iron–steel manufacturers. The highest loadings of La and Ce were also found on this factor, which is supported by observed enrichments of rare earth elements in emissions from iron–steel facilities (Geagea et al., 2007). The La/Ce ratios in Underhill precipitation samples were also consistent with the predicted average continental crustal composition (Olmez and Gordon, 1985; Fig. SI-2). Given past aerosol analysis at Underhill (Gao et al., 2006), this could suggest an additional influence from long-range windblown dust.

The coal combustion factor was characterized by the highest contributions of S, As, and Se (Grahame and Hidy, 2004), and identification of this source corresponded with the event As/Se and S/Se ratios (Fig. SI-3). 77% of samples displayed As/Se < 1, signifying coal combustion emissions (Olmez et al., 1998). Furthermore, the S/Se slope for event wet deposition was 2630 ($R^2 = 0.75$), following the prediction that S/Se is typically <1000 in CFUB emissions and approaches a steady state value of ~3000 downwind of CFUBs as emitted SO_2 is slowly converted to sulfate during transport (Tuncel

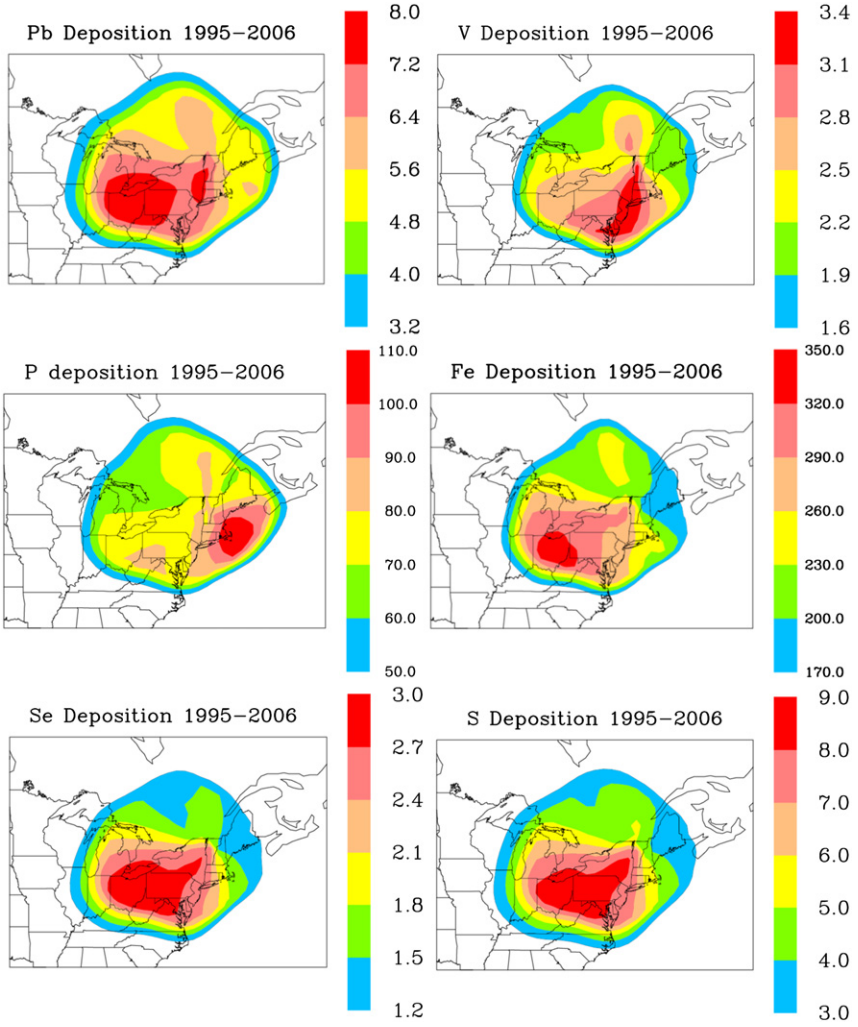

Fig. 4. QTBA of Pb, V, P, Fe, Se (μg m^{-2}) and S (mg m^{-2}) wet deposition at Underhill, VT from 1995 to 2006.

et al., 1985). PMF attributed ~60% of the total Hg deposition to this factor for the 12-year period, and attributed 50–70% of Hg deposition to this factor annually. The percent contribution to Hg deposition was highest in the summer (70%) and lowest in the winter (50%), due in part to meteorological transport patterns at the Underhill site (Gratz et al., 2009). The estimated event coal combustion contributions correspond closely with the measured deposition amounts, wherein the largest estimated contributions to event Hg deposition from CFUBs occurred during summer months and the model estimated contributions clearly did not decline over time (Fig. 3). PMF also consistently indicated coal combustion as the dominant contributor (~60%) to Hg deposition in both six-year periods (1995–2000, 2001–2006). The contribution to Hg deposition at Underhill from CFUBs was comparable to the PMF analysis of precipitation samples from the highly-industrialized Steubenville, OH site in the Midwestern U.S., where ~70% of Hg wet deposition was attributed to CFUB emissions based on elevated S and Se loadings (Keeler et al., 2006). The finding that CFUBs were consistently the largest source of Hg in Underhill precipitation supports the previous observation that total annual Hg wet deposition did not decline from 1995 to 2006 due to consistent transport of Hg from the high emission source areas in the Midwest and East Coast where the density of CFUBs is largest (Fig. 1) (Gratz et al., 2009).

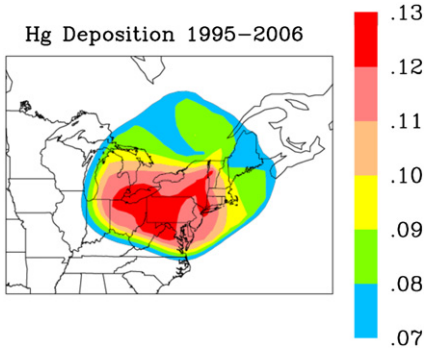

Fig. 5. QTBA of Hg wet deposition (μg m^{-2}) at Underhill, VT from 1995 to 2006.

These findings are important given the projected declines in Hg deposition following waste incinerator emission reductions in the 1990s; however, the relative impact of regional Hg sources is consistent with our understanding of Hg speciation in emissions. Given that RGM tends to deposit close to emission sources (Lin and Pehkonen, 1999; White et al., 2009), it should not be readily available for regional transport. RGM comprises ~75% and ~95% of Hg in municipal and medical waste incinerator emissions, respectively (Carpi, 1997; Dvonch et al., 1999). In contrast, Hg emitted from CFUBs can be ~50–80% RGM, and ~20–50% Hg^0 (Carpi, 1997; Seigneur et al., 2006). Although a large portion of RGM

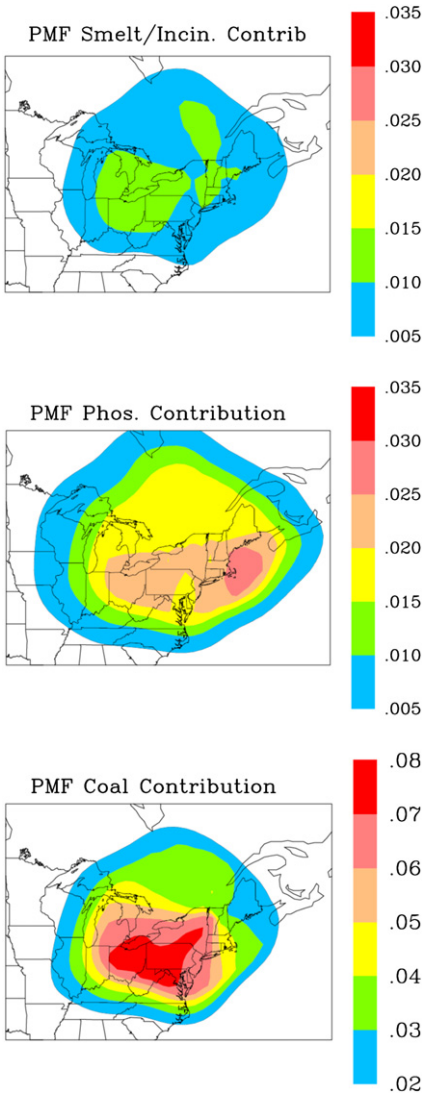

Fig. 6. QTBA of PMF estimated contributions to Hg wet deposition (μg m^{-2}) at Underhill, VT from 1995 to 2006.

emissions are expected to be removed through near-field deposition (White et al., 2009), the relative amount of RGM in CFUB emissions available for downwind transport should be greater than that in waste incinerator emissions. Furthermore the relatively taller stack releases from many CFUBs compared to those of waste incinerators may facilitate longer RGM transport distances, especially at times when the mixed layer is below the stack height. This may be particularly important at Underhill where the site elevation increases the potential for intercepting source emissions transported above the mixed layer (Vermont ANR, 2008). In summary, because there are no major municipal or medical waste incinerators within 100 km, waste incinerator emissions should not substantially influence Hg deposition at Underhill, whereas other regional combustion sources (e.g. CFUBs) should have a greater influence.

4.2. QTBA

4.2.1. QTBA of trace element wet deposition

The application of QTBA to select trace elements showed coherence with the known locations of major emission point sources, demonstrating that QTBA was capable of distinguishing between source regions. For example, QTBA attributed Pb deposition to several source regions (Fig. 4), including a Midwest contribution coinciding with the locations of CFUBs and iron–steel manufacturers. The smaller contributions north of the site pointed to Canadian smelters, whereas the elevated contributions from eastern New York were likely due to large cement production facilities near the Albany and downstate areas (Fig. 1).

In contrast, the contribution field for V deposition (Fig. 4) was greatest along the East Coast through New York and New Jersey where major oil-fired utility boilers are located and residual oil burning is common. Additionally, V deposition revealed a Midwestern contribution related to CFUB emissions (Tuncel et al., 1985; Grahame and Hidy, 2004).

QTBA clearly indicated that the highest contributions to P (Fig. 4) and K (not shown) were associated with east-southeasterly flow. This could suggest a regional wood-burning source, but is also consistent with hypothesized contributions from fertilizer application in the northeast. Although QTBA seemed to suggest a marine source of P, collocated AIRMoN samples generally do not indicate a relationship between Na^+ or Cl^- with PO_4 or K^+ (NADP AIRMoN). The modeled transport direction, combined with the observed seasonality in the phosphorus source contribution, may also suggest the impact of Nor'easter storms which typically occur in fall, winter, and spring.

QTBA also consistently suggested that the dominant sources of Fe (Fig. 4) and other elements apportioned to the iron–steel factor (e.g. Mg, La, and Ce (not shown)) were located in the Midwest, predominantly in Ohio, southeast Michigan, and western Pennsylvania. The identified source regions strongly coincide with known locations of regional iron–steel manufacturers (Fig. 1).

Finally, QTBA suggested a very strong Midwest contribution to Se and S deposition (Fig. 4). These elements are known tracers of coal combustion (Tuncel et al., 1985; Wen and Carignan, 2007) and the QTBA contribution fields distinctly point to the region's largest density of CFUBs.

4.2.2. QTBA of Hg wet deposition

The QTBA modeled Hg deposition from 1995 to 2006 (Fig. 5) was highly similar to the patterns for S and Se (Fig. 4) with the most likely source regions located in the Midwest and Ohio River Valley. Contributions could also be observed south–southeast of the site which were similar to the regions identified for Pb and P. However, the strong relationship between Hg, S and Se in PMF suggested that the most dominant Hg source region was southwest of Underhill. QTBA of Hg deposition in the two six-year periods (1995–2000 and 2001–2006; Fig. SI-4) also consistently identified the Midwest as the dominant source region of Hg at Underhill during both time periods. The consistent pattern of Hg deposition with known coal combustion tracers (S and Se) supports the hypothesis that CFUBs are the largest sources of Hg in Underhill precipitation.

4.2.3. QTBA of PMF estimated source contributions to Hg wet deposition

The contribution to Hg deposition from the smelter/incinerator factor showed that the likely sources were located in Canada, the Midwestern U.S., and the Northeastern U.S (Fig. 6). This was similar to the regions identified for Pb deposition in QTBA and coincided with the high loadings of Pb on the PMF smelter/incinerator factor. These source regions also pointed to major metal smelters in the Midwest and Canada, as well as municipal waste incinerators in the Northeast (Fig. 1).

Similarly to the QTBA plot of P deposition, Hg deposition associated with the phosphorus source suggested predominantly southeasterly transport from the New England coast, confirming a distinct transport direction associated with this source (Fig. 6). In

this region, the most likely sources of Hg with contributions of P and K are biomass burning and fertilizer application; however, further analyses are needed to more confidently interpret this source. Consistent with Gratz et al. (2009), PMF and QTBA suggested relatively small contributions to Hg deposition under northerly and easterly transport, which often bring cold temperatures and snow or mixed precipitation.

The PMF contribution to Hg deposition from the coal combustion factor suggested transport of emissions from the Midwest (Fig. 6). The contours associated with the highest Hg deposition from coal combustion were nearly identical to the patterns for S and Se, confirming a common source of these elements as well as the use of S and Se as tracers of coal combustion.

5. Conclusions

The PMF multivariate statistical model results suggest that the major sources of Hg in wet deposition at Underhill, VT from 1995 to 2006 were CFUBs, a combination of non-ferrous metal smelters and waste incinerators, and a mixture of wood-burning and fertilizer application. Although waste incineration was previously a significant anthropogenic Hg source, our analysis suggests that emission reductions in the mid-1990s did not substantially reduce Hg wet deposition at Underhill. This occurred, in part, because the dominance of RGM in waste incinerator Hg emissions prohibits long-range transport of Hg. Instead, the model clearly indicates that CFUB emissions were consistently the largest contributing source of Hg. Furthermore, QTBA of Hg and trace element deposition is consistent with the known locations of major source types. The dominant contribution from Midwest CFUBs to Hg deposition at Underhill is consistent with past findings that the largest Hg deposition amounts at Underhill occurred with southwesterly transport. The combined results of PMF and QTBA provide strong corroborative evidence supporting the finding that total annual Hg wet deposition at Underhill did not decline from 1995 to 2006 due to consistent transport of Midwestern CFUB Hg emissions.

Acknowledgments

This research was sponsored by the Cooperative Institute of Limnology and Ecosystem Research (CILER) under cooperative agreements from the Environmental Research Laboratory (ERL), the National Oceanographic and Atmospheric Administration (NOAA), and the U.S. Department of Commerce. The U.S. EPA Great Waters Program, the Northeast States for Coordinated Air Management (NESCAUM), EPA Region I, and EPA-ORD-HEASD provided additional support. We acknowledge assistance from Dr. Tim Scherbatskoy during the formative years of this study, as well as the hard work and dedication of site operators Carl Waite and Miriam Pendleton. We thank the past and present UMAQL members for their dedicated support and contributions to this research. We also acknowledge our collaborators from the State of Vermont, U.S. EPA, NOAA, and NESCAUM. Finally, we thank the anonymous reviewers for their thoughtful comments, questions, and suggestions.

This manuscript is dedicated to the memory of co-author Dr. Gerald J. Keeler. Jerry made this project possible from start to finish with his attention to detail and his commitment to conducting the best scientific research possible. He was a valued colleague, advisor, and friend, and he will be sorely missed.

Appendix. Supplementary information

Supplementary information associated with this article can be found, in the online version, at doi:10.1016/j.atmosenv.2011.07.001.

References

Anttila, P., Paatero, P., Tapper, U., Järvinen, O., 1995. Source identification of bulk wet deposition in Finland by Positive Matrix Factorization. Atmospheric Environment 29 (14), 1705–1718.

Burke, J., Hoyer, M., Keeler, G.J., Scherbatskoy, T., 1995. Wet deposition of mercury and ambient mercury concentrations at a site in the Lake Champlain basin. Water, Air, and Soil Pollution 80, 353–362.

Burke, J.M., 1998. An Investigation of Source-Receptor Relationships for Atmospheric Mercury in the Great Lakes Region Using Receptor Modeling Techniques. Ph.D. Dissertation, University of Michigan.

Butler, T.J., Cohen, M.D., Vermeylen, F.M., Likens, G.E., Schmeltz, D., Artz, R.S., 2008. Regional precipitation mercury trends in the eastern USA, 1998–2005: declines in the Northeast and Midwest, no trend in the Southeast. Atmospheric Environment 42, 1582–1592.

Carpi, A., 1997. Mercury from combustion sources: a review of the chemical species emitted and their transport in the atmosphere. Water, Air, and Soil Pollution 98, 241–254.

Cohen, M.D., Artz, R.S., Draxler, R.R., 2007. Report to Congress: Mercury Contamination in the Great Lakes. NOAA Air Resources Laboratory, Silver Spring, MD.

Draxler, R.R., Hess, G.D., 1997. Description of the HYSPLIT_4 Modeling System. NOAA TECHNICAL MEMORANDUM ERL ARL-224.

Dvonch, J.T., Graney, J.R., Keeler, G.J., Stevens, R.K., 1999. Use of elemental tracers to source apportion mercury in south Florida precipitation. Environmental Science and Technology 33, 4522–4527.

Environment Canada, 2007. National Pollutant Release Inventory (NPRI). www.ec.gc.ca/inrp-npri/.

Erich, M.S., Ohno, T., 1992. Phosphorus availability to corn from wood ash-amended soils. Water, Air, and Soil Pollution 64, 475–485.

Evers, D.C., Han, Y.-J., Driscoll, C.T., Kamman, N.C., Goodale, M.W., Lambert, K.F., Holsen, T.M., Chen, C.Y., Clair, T.A., Butler, T., 2007. Biological mercury hotspots in the northeastern United States and southeastern Canada. BioScience 57, 29–43.

Gao, N., Gildemeister, A.E., Krumhansl, K., Lafferty, K., Hopke, P.K., Kim, E., Poirot, R.L., 2006. Sources of fine particulate species in ambient air over Lake Champlain basin, VT. Journal of Air and Waste Management Association 56, 1607–1620.

Geagea, M.L., Stille, P., Perrone, Th, 2007. REE characteristics and Pb, Sr, and Nd isotopic compositions of steel plant emissions. Science of the Total Environment 373, 404–419.

Grahame, T., Hidy, G., 2004. Using factor analysis to attribute health impacts to particulate pollution sources. Inhalation Toxicology 16 (Suppl. 1), 143–152.

Gratz, L.E., Keeler, G.J., Miller, E.K., 2009. Long-term relationships between mercury wet deposition and meteorology. Atmospheric Environment 43, 6218–6229.

Hammerschmidt, C.R., Fitzgerald, W.F., 2006. Methylmercury in freshwater fish linked to atmospheric mercury deposition. Environmental Science and Technology 40, 7764–7770.

Hammond, D.M., Dvonch, J.T., Keeler, G.J., Parker, E.A., Kamal, A.S., Barres, J.A., Yip, F.Y., Brakefield-Caldwell, W., 2008. Sources of ambient fine particulate matter at two community sites in Detroit, MI. Atmospheric Environment 42, 720–732.

Juntto, S., Paatero, P., 1994. Analysis of daily precipitation data by Positive Matrix Factorization. Environmetrics 5 (2), 127–144.

Kahl, J.D., Samson, P.J., 1986. Uncertainty in trajectory calculations due to low resolution meteorological data. Journal of Climate and Applied Meteorology 25, 1816–1831.

Keeler, G.J., Samson, P.J., 1989. Spatial representativeness of trace element ratios. Environmental Science and Technology 23, 1358–1364.

Keeler, G.J., Gratz, L.E., Al-Wali, K., 2005. Long-term atmospheric mercury wet deposition at Underhill, Vermont. Ecotoxicology 14, 71–83.

Keeler, G.J., Landis, M.S., Norris, G.A., Christianson, E.M., Dvonch, J.T., 2006. Sources of mercury wet deposition in Eastern Ohio, USA. Environmental Science and Technology 40, 5874–5881.

Landis, M.S., Keeler, G.J., 1997. Critical evaluation of a modified automatic wet-only precipitation collector for mercury and trace element determinations. Environmental Science and Technology 31, 2610–2615.

Landis, M.S., Keeler, G.J., 2002. Atmospheric mercury deposition to Lake Michigan during the Lake Michigan Mass Balance Study. Environmental Science and Technology 36, 4518–4524.

Lin, C., Pehkonen, S.O., 1999. The chemistry of atmospheric mercury. Atmospheric Environment 33, 2067–2079.

Liu, B., 2007. Atmospheric Mercury Speciation in Urban Air: Identifying the Relative Importance of Local Anthropogenic Sources in Detroit, Michigan. Ph.D. Dissertation, University of Michigan.

Liu, W., Hopke, P.K., Han, Y., Yi, S., Holsen, T.M., Cybart, S., Kozlowski, K., Milligan, M., 2003. Application of receptor modeling to atmospheric constituents at Potsdam and Stockton, NY. Atmospheric Environment 37, 4997–5007.

Machemer, S.D., 2004. Characterization of airborne bulk particulate from iron and steel manufacturing facilities. Environmental Science and Technology 38, 381–389.

Mahowald, N., Jickells, T.D., Baker, A.R., Artaxo, P., Benitez-Nelson, C.R., Bergametti, G., Bond, T.C., Chen, Y., Cohen, D.D., Herut, B., Kubilay, N., Losno, R., Luo, C., Maenhaut, W., McGee, K.A., Okin, G.S., Siefert, R.L., Tsukuda, S., 2008. Global distribution of atmospheric phosphorus sources, concentrations and deposition rates, and anthropogenic impacts. Global Biogeochemical Cycles 22, GB4026.

Mamane, Y., Pirrone, N., 1998. Vanadium in the atmosphere. In: Nriagu, J.O. (Ed.), Vanadium in the Environment. Part 1: Chemistry and Biochemistry. John Wiley & Sons, Inc., New York, pp. 37–72.

Morishita, M., Keeler, G.J., Wagner, J.G., Harkema, J.R., 2006. Source identification of ambient PM2.5 during summer inhalation exposure studies in Detroit, MI. Atmospheric Environment 40, 3823–3834.

National Atmospheric Deposition Program (NADP) AIRMoN Precipitation Data. http://nadp.sws.uiuc.edu/AIRMoN/amData.aspx.

New England Interstate Water Pollution Control Commission (NEIWPCC), 2007. Northeast Regional Mercury Total Maximum Daily Load (http://www.neiwpcc.org/mercury/mercury-docs/FINAL%20Northeast%20Regional%20Mercury%20TMDL.pdf).

Norris, G., Vedantham, R., Wade, K., Brown, S., Prouty, J., Foley, C., 2008. EPA Positive Matrix Factorization (PMF) 3.0 Fundamentals & User Guide. U.S. Environmental Protection Agency.

Northeast States for Coordinated Air Use Management (NESCAUM), 2005. Inventory of Anthropogenic Mercury Emissions in the Northeast. http://www.nescaum.org/documents/inventory-of-anthropogenic-mercury-emissions-in-the-northeast/ November 30, 2005 Report.

Olmez, I., Gordon, G.E., 1985. Rare earths: atmospheric signatures for oil-fired power plants and refineries. Science 229, 966–968.

Olmez, I., Sheffield, A.E., Gordon, G.E., Houck, J.E., Pritchett, L.C., Cooper, J.A., Dzubay, T.G., Bennett, R.L., 1988. Compositions of particles from selected sources in Philadelphia for receptor modeling applications. JAPCA 38, 1392–1402.

Olmez, I., Ames, M.R., Gullu, G., 1998. Canadian and U.S. sources impacting the mercury levels in fine atmospheric particulate material across New York State. Environmental Science and Technology 32, 3048–3054.

Paatero, P., 1997. Least squares formulation of robust non-negative factor analysis. Chemometrics and Intelligent Laboratory Systems 37, 23–35.

Paatero, P., Tapper, U., 1994. Positive Matrix Factorization – a nonnegative factor model with optimal utilization of error-estimates of data values. Environmetrics 5 (2), 111–126.

Pitman, R.M., 2006. Wood ash use in forestry – a review of the environmental impacts. Forestry 79 (5), 563–588.

Poirot, R.L., Wishinski, P.R., Hopke, P.K., Polissar, A.V., 2001. Comparative application of multiple receptor methods to identify aerosol sources in northern Vermont. Environmental Science and Technology 35, 4622–4636.

Polissar, A.V., Hopke, P.K., Poirot, R.L., 2001. Atmospheric aerosol over Vermont: chemical composition and sources. Environmental Science and Technology 35, 4604–4621.

Rahn, K.A., Lowenthal, D.H., 1984. Elemental tracers of distant regional pollution aerosols. Science 223 (4632), 132–139.

Schroeder, W.H., Munthe, J., 1998. Atmospheric mercury – an overview. Atmospheric Environment 32, 809–822.

Seigneur, C., Lohman, K., Vijayaraghavan, K., Jansen, J., Levin, L., 2006. Modeling atmospheric mercury deposition in the vicinity of power plants. Journal of Air and Waste Management Association 56, 743–751.

Tuncel, S.G., Olmez, I., Parrington, J.R., Gordon, G.E., 1985. Composition of fine particle regional sulfate component in Shenandoah Valley. Environmental Science and Technology 19, 529–537.

U.S. Environmental Protection Agency (U.S. EPA), 1997. Mercury Study Report to Congress, vol. 2. Office of Air Quality Planning and Standards, Office of Research and Development, Washington DC. EPA-452/R-97–003.

U.S. Environmental Protection Agency (U.S. EPA), 2002. National Emissions Inventory (NEI) on Planet Hazard. http://www.planethazard.com.

U.S. Environmental Protection Agency (U.S. EPA), 2005. National Emissions Inventory (NEI) Data and Documentation. www.epa.gov/ttnchie1/net/2005inventory.html.

Vance, E.D., 1996. Land application of wood-fired and combination boiler ashes: an overview. Journal of Environmental Quality 25, 937–944.

Vermont Agency of Natural Resources (ANR), 2008. Department of Environmental Conservation: Air Pollution Control Division. Final Report: Air Quality Data and Observations Made in Vermont during the November 2006 Trial Burn of Tire Derived Fuel at the International Paper Company, Ticonderoga, New York (http://www.anr.state.vt.us/air/docs/FinalReportComplete.pdf).

Wen, H., Carignan, J., 2007. Reviews on atmospheric selenium: emissions, speciation, and fate. Atmospheric Environment 41, 7151–7165.

White, E.M., Keeler, G.J., Landis, M.S., 2009. Spatial variability of mercury wet deposition in eastern Ohio: summertime meteorological case study analysis of local source influences. Environmental Science and Technology 43, 4946–4953.

Zhou, L., Hopke, P.K., Liu, W., 2004. Comparison of two trajectory based models for locating particle sources for two rural New York sites. Atmospheric Environment 38, 1955–1963.